Effect of multiple impeller designs and configurations on the droplet size and uniformity in a 100 L scale stirred tank

Jeil Park*, Wooyoul Ahan**, and Jae W. Lee*,†

*Department of Chemical and Biomolecular Engineering, KAIST, 291 Daehak-ro, Yuseong-gu, Daejeon 34141, Korea
**Hanwha Solutions R&D Institute, 76 Gajeong-ro, Yuseong-gu, Daejeon 34128, Korea

Abstract−This study investigated the effect of multiple impeller designs and configurations on the Sauter mean diameter and the uniformity of droplet size in a 100 L scale stirred tank. By using a borescope installed inside the tank, droplet images of a highly turbid liquid-liquid system were captured even at high impeller speeds, and by adjusting the borescope position, it could be observed how the droplet size changed depending on the position. The area of the flow pattern produced by the impeller was taken as an impeller region, and it explained well the change in the droplet size due to the varying liquid phase volume and impeller spacing. In addition, the change of the Sauter mean diameter and the droplet size uniformity was also elucidated by the variation of the impeller diameter, blade angle, and number of impellers. All three parameters showed a decrease in the deviation between droplet sizes as they increased, but increasing the impeller diameter was the most effective in reducing the Sauter mean diameter itself.

Keywords: Borescope, Droplet Size Uniformity, Multiple Impellers, Sauter Mean Diameter, Stirred Tank

INTRODUCTION

Multiphase reactions have been utilized in various biphasic [1-4] and triphasic [5] reactors because of product turnovers that were improved by the facilitation of mass and heat transfer. A stirred tank has specifically been used in various reactive processes of chemical and biochemical fields [6-9]. When two immiscible liquids are used as reactants, one liquid phase is dispersed into the other by mechanical agitation, and droplets sre formed. Since both reaction and mass transfer take place at the interface between the droplet and the liquid phase, there has been much research on the droplet size [8,10-13].

However, previous studies mainly used a lab-scale stirred tank, so only a single impeller was used [8,12,14]. A single impeller system is sufficient for such small scale reactors, but it is common to use a multiple impeller system when the size or height of the reactor vessel is large [15-18]. In particular, in the dual impeller configuration, the use of a pitched paddle as an upper impeller has high hydraulic efficiency [19], and an impeller that produces axial flow is frequently employed with other impellers [20]. In this case, using multiple sampling locations makes it possible to investigate in detail the effect of the geometry and type of each impeller on the size of the droplets located near the impeller.

Another factor considered important in a stirred tank is to secure a uniform droplet size using multiple impellers [21]. Since the surface area of the droplets is a key factor for reaction or mass transfer, the Sauter mean diameter is an essential factor for evaluating the productivity of the stirred tank. However, the Sauter mean diameter does not provide any information about the droplet size deviation at the sampling locations [13]. Thus, the Sauter mean diameter and the droplet size distribution should be considered together to properly understand the droplet breakup behaviors according to the changes in geometry in the stirred tank. If the changes in droplet size and its uniformity can be predicted, it will be of great help in determining the operating conditions of the PVC polymerization process, by which the droplet size and distribution have a significant impact on the processing and performance of the final product [22]. However, since previous studies mainly used a single impeller and one sampling location [14,23], it is difficult to apply their results to a multiple impeller system, which could make a deviation in the droplet size according to the location.

In this study, a stirred tank with 100 liters and various multiple impeller designs and configurations were used to investigate the change of the Sauter mean diameter and uniformity of the droplet size with respect to the sampling locations. First, the change in the droplet size by reducing the liquid phase volume was investigated. Next, impeller spacing was varied with the liquid phase volume fixed to see how the relative position between the impellers affects the droplet size. Finally, the effect of the impeller diameter, blade angle, and the number of impellers on the Sauter mean diameter and the droplet size uniformity was examined.

For the droplet size measurement, a borescope method was used. Since the borescope is directly inserted into the reactor, it is less distorted than when exterior shooting is used for the turbid liquid-liquid system, and it is possible to take images of droplets with a diameter of 30-1,000 μm [24]. In addition, because the diameter of the borescope is much smaller than that of the reactor, inserting it inside the reactor does not have a significant effect on the internal flow [12]. It is also suitable for obtaining data on the droplet sizes by location, since it can move freely up and down within the reac-

Table 1. The properties of the aqueous and organic liquids at 25 °C

Substance	Density (g/cm³)	Surface tension (mN/m)	Viscosity (cP)	Interfacial tension (mN/m)
Water	0.997	71.976	0.890	28.43
1,2-Dichloroethane	1.245	31.860	0.779	

tor. Information on the Sauter mean diameter and the droplet size uniformity measured in different regions for these various impeller designs and configurations is essential for predicting the droplet breakup behavior and choosing the proper impeller design in a multi-impeller stirred tank.

## EXPERIMENTAL SECTION

1. Materials

For two immiscible liquids, tap water and 1,2-dichloroethane (DCE, extra pure grade, 99.0%, SAMCHUN Pure Chemicals, Korea) were used. The properties of the two liquid phases are presented in Table 1. The density and viscosity of the water was obtained from Rumble et al. [25] and Laliberté et al. [26], respectively. The surface tension of the water was calculated by the equation of Vargaftik et al. [27]. The properties of DCE were obtained from Rumble et al. [25], and for the interfacial tension between water and DCE, the experimental value of Girault et al. [28] was used. Since the density of the organic phase was quite high, 1.245 g/cm³, the droplet size data obtained in this study will be useful for understanding the droplet breakup behavior under conditions in which the organic phase density is higher than that of the aqueous phase.

2. Experimental Setup

The experimental apparatus is illustrated in Fig. 1. A dished-bottom stirred tank with a 40 cm diameter and a 80 cm height (cylinder part) was used to measure the droplet size, and the height of the dished part was 10 cm. To prevent vortexing of the liquid phase, twelve cylindrical baffles with a diameter of 2 cm were placed, and the distance from the reactor center to each baffle was 12 cm. A heating jacket was used to maintain a constant temperature during

the measurement, and the temperature difference from the set point was kept within ±1 °C. For capturing the droplet images, a borescope was inserted into the stirred tank through a 1/2 inch stainless steel tube. A small size borescope was used (94 cm length, 0.72 cm diameter; Gradient Lens Corporation, Hawkeye Pro Super Hardy, USA) since the internal flow is affected more as the size of the borescope becomes larger. The borescope was directly connected to a CCD camera (Sony, XCD-U100, Japan), and it was also connected to a flashlight (Excelitas Technologies, X-1500, USA) through a light guide. Thus, sufficient light could be delivered even though the shutter speed was fast. In addition, to prevent damage to the borescope due to backflow of the liquid phase, a lens (12.5 mm diameter, 1.75 mm thickness; Edmund optics, BOROFLOAT® Borosilicate Windows, USA) was attached to the end of the stainless steel tube. To investigate the change of the droplet size by location, three sampling locations were used for the droplet image shooting as shown in Fig. 1. Ports 1 and 3 were placed at the same height as the center of the upper and lower impellers, respectively, and port 2 was placed halfway between the other two.

For the impellers, a three-bladed stainless paddle impeller (11.15-11.65 cm diameter, and 3.7 cm blade width as shown in Fig. 2(a)) and a three-bladed stainless pitched paddle (10° blade angle, 11.15 cm diameter, and 3.7 cm blade width as shown in Fig. 2(b)) were used. Table 2 presents the configuration and the geometry of the impellers used. Since there has never been a mixed use of these different types of impeller for all experimental conditions, the impeller geometry for the multiple impeller was not duplicated, but the number of impellers used for each condition (N_I) is specified instead (Table 2).
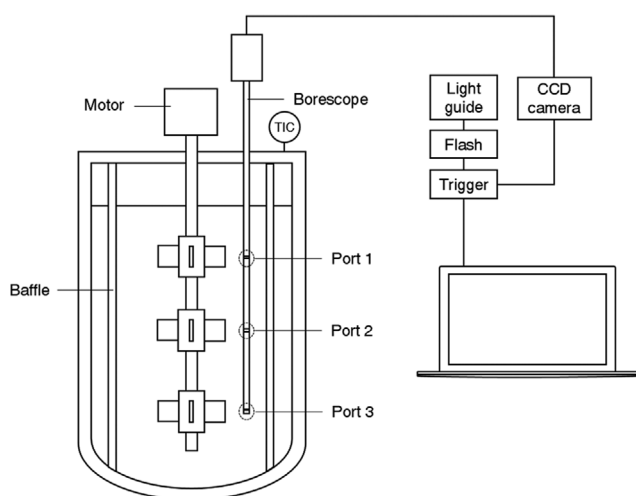
Fig. 1. Schematic diagram of the experimental apparatus (here, only a three stage paddle impeller is illustrated).
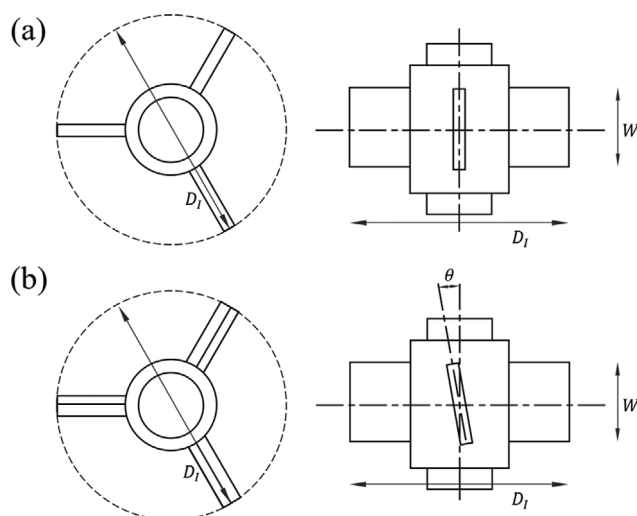
Fig. 2. Schematic diagram of the different types of impellers used in this work: (a) Paddle impeller; (b) pitched paddle impeller.

Table 2. Geometric dimensions of the impellers used in this study

No.	D_I/D	W/D_I	θ (°)	V (L)*	S/D*	T/D*	B/D*	N_I*
1	0.28	0.33	0	80	0.675	0.318	0.438	2
2	0.28	0.33	0	69	0.475	0.318	0.438	2
3	0.28	0.33	0	64	0.350	0.318	0.438	2
4	0.28	0.33	0	80	0.550	0.443	0.438	2
5	0.28	0.33	0	80	0.613	0.380	0.438	2
6	0.28	0.33	0	80	0.638	0.355	0.438	2
7	0.28	0.33	0	80	0.700	0.293	0.438	2
8	0.28	0.33	0	80	0.738	0.255	0.438	2
9	0.29	0.32	0	80	0.675	0.318	0.438	2
10	0.28	0.33	10	80	0.675	0.318	0.438	2
11	0.28	0.33	0	80	0.338	0.318	0.438	3

*V: liquid phase volume, S: impeller spacing, T: top clearance of the upper impeller, B: bottom clearance of the lower impeller, and N_I: number of impellers.

3. Borescope System Calibration

Calibration is necessary to calculate the actual size of the droplets obtained by the borescope system. Therefore, three glass beads whose sizes were already known were used (diameter of 0.25 mm, SUPELCO, USA; diameter of 2.0 mm, Glastechnique, Germany, and diameter of 0.075 mm, SUPELCO, USA). Before acquiring the glass bead image, the focal distance of the CCD camera was carefully adjusted to obtain a clear borderline when the glass bead was placed just in front of the lens. For the reliable data, it is known that over 200 glass beads need to be included in the measurement [12,24]. After a photograph was taken of the glass beads, each size of glass bead was determined in pixels in the Adobe Photoshop™ program. Using the average pixel of the glass bead images and the diameter of the actual glass bead, the size of 1 pixel was calculated. To confirm whether the size of 1 pixel varied depending on the size of the target object, the values obtained from three glass bead sets were compared, and the mean of the three values was used as a reference size for the further experiments (measured droplet sizes in pixels were converted into actual sizes in micrometers).

4. Experimental Procedure

The droplet size was measured at 25 °C and an impeller speed of 320-600 rpm. Since the minimum Reynolds number was 8.40×10^4 (at the lowest impeller speed of 320 rpm), the fluid flow was under the turbulent regime for all the experimental conditions.

The total liquid phase volume of 80 L was selected as a base case. To investigate the effect of the liquid phase volume reduction, 64 and 69 L of liquid phase volume were selected since the aspect ratio H/D (charged liquid phase height/reactor diameter) for the two was 1.1 and 1.2, respectively. However, the organic phase holdup fraction was fixed to 0.375 during the experiment. After the required aqueous and organic phase for each liquid phase volume (e.g., 50 L of aqueous phase and 30 L of organic phase were used for the 80 L experiment) was carefully poured, the agitation was started with a prescribed impeller speed. For the experiment where the liquid phase volume changed, the power per volume (P/V) at 80 L was used to make the P/V fixed. So, the impeller speeds to maintain the same P/V were calculated by Eq. (1), and the results are shown in Table 3.

Table 3. Impeller speeds for equal P/V at different liquid phase volumes

Impeller speed at 80 L (rpm)	Impeller speeds for equal P/V	
	at 64 L (rpm)	at 69 L (rpm)
400	320	345
500	400	431
600	480	518

$$P = 2\pi NM \tag{1}$$

Since the impeller spacing also decreases when the liquid phase volume reduces, it is difficult to investigate the effect of one factor alone. Therefore, the Sauter mean diameter with various impeller spacings (14.0-29.5 cm) was measured by moving the upper impeller up and down, while maintaining the liquid phase volume at 80 L.

The effect of the dual impeller diameter and the blade angle on the droplet size was also investigated. When the impeller speed increased, the droplet size reduction effect was significant at a relatively low impeller speed. However, when the impeller speed increased above a certain value, the droplet size did not change much [8,29]. Thus, it was investigated that whether an increase in the impeller diameter from 11.15 to 11.65 cm would cause an additional droplet breakup, when the droplet size was already sufficiently decreased. In addition, the effect of an increasing impeller diameter on the decrease of the Sauter mean diameter at port 2 (which was expected to be the least affected by the two impellers at ports 1 and 3) was also investigated. For the impeller blade angle, the two paddle impellers were replaced with two 10° pitched paddle impellers to determine whether the droplet size uniformity could be enhanced without making the droplet size too large. Finally, the number of the impeller was increased to three to investigate its effect on the Sauter mean diameter and the droplet size uniformity.

Although a droplet stabilization time of 10 min is known to be sufficient when conducting the droplet size measurement [12], the appropriate stabilization time (see Fig. S1 in the Supplementary Mate-

rial) was checked since the reactor used in this study was larger than that of the previous studies [8,12]. In our study, the droplet image started to be taken 20 min after the droplet stabilization time. In addition, it is known that 200 droplets are sufficient for the statistically reliable data [12,24]. However, an experiment was conducted to verify whether the Sauter mean diameter did not change significantly when more than 200 droplets was used (see Fig. S2 in the Supplementary Material) and confirmed that 200 droplets were enough.

The position of the borescope was adjusted when the impeller spacing was changed, so that ports 1 and 3 were always located next to the impellers and port 2 was located halfway between the two. If three impellers were used, each sampling location was placed next to the three impellers. The size of the droplets taken by the borescope system was measured in pixels through the Adobe Photoshop program and converted to the actual size using the values obtained by the borescope calibration. Using the droplet sizes, the Sauter mean diameter was calculated, as presented in Eq. (2). The experiment was conducted three times in total and the average value was set as the final Sauter mean diameter.

$$d_{32} = \frac{\Sigma_i n_i d_i^3}{\Sigma_i n_i d_i^2} \qquad (2)$$

RESULTS AND DISCUSSION

1. Sauter Mean Diameter Measurement at Different Liquid Phase Volumes

To investigate the effect of the liquid phase volume on the droplet size, the liquid phase volume was reduced and the Sauter mean diameter was measured. However, the top clearance of the upper impeller and the bottom clearance of the lower impeller were fixed while the liquid volume varies. Thus, both the liquid phase volume and the impeller spacing decreased in this case. Examples of the actual droplet image are shown in Fig. 3.

In Fig. 4, the Sauter mean diameters with different liquid phase volumes are presented. For convenience, the impeller speeds indicated on the x-axis were the impeller speeds at the liquid phase volume of 80 L. For 64 and 69 L, the impeller speeds calculated in Section 2.4 were used (refer to Table 3). Here, since the P/V was always the same regardless of the liquid phase volume, the Sauter
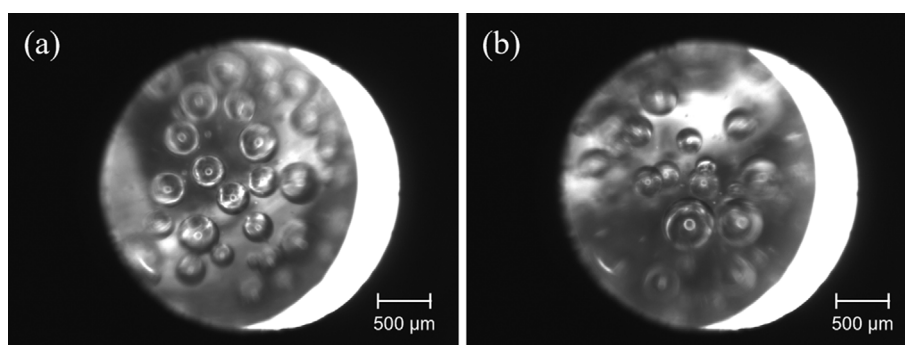

Fig. 3. Droplet image obtained by the borescope system at port 1, 400 rpm; (a) 11.15 cm paddle-paddle dual impeller; (b) 11.15 cm 10° pitched-pitched dual impeller.
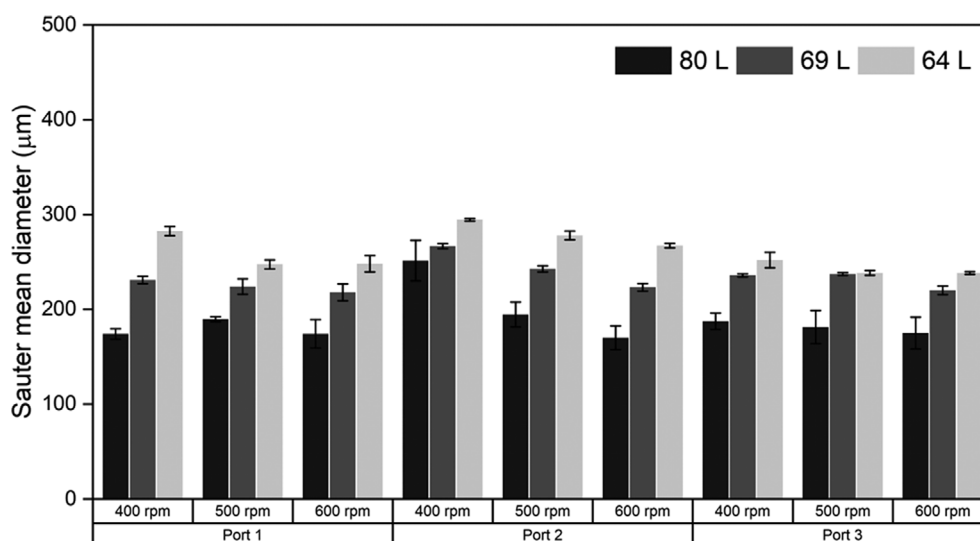

Fig. 4. Measured Sauter mean diameters with different liquid phase volumes (here, only the impeller speed at the liquid phase volume of 80 L was displayed for convenience).

mean diameter should not change much considering the constant P/V has been used as a scale-up criterion [13,30]. Surely, it should be taken into account that the general scale-up study was conducted under geometrically similar conditions (e.g., constant D_I/D ratio, constant H/D, etc.) and it dealt with the large change in the reactor size [31]. The experiment conducted in this study did not satisfy all those conditions, since the diameter of the impeller and the reactor remained unchanged. However, since the liquid phase volume did not change much from 80 to 69 L at the same diameter of 40 cm, it did not deviate significantly from the geometrically similar conditions (H/D reduced by 13.99%). Consequently, the significant increase in the Sauter mean diameter at the reduced liquid phase volume implies that the equal P/V does not help much to obtain the same Sauter mean diameter. Since the P/V is directly proportional to the mean energy dissipation rate ($\bar{\varepsilon} = \dfrac{P}{\rho V}$), these results are consistent with the previous studies [32-34] in which the equal mean energy dissipation rate was inappropriate for the scale-up criterion.

The constant P/V did not fit well for the scale-up criteria was probably because the impeller power was not dispersed evenly throughout the whole liquid mixture. In the vicinity of the impeller, droplet breakup occurred frequently, but this effect decreased as the droplets moved away from the impeller. Thus, an attempt was made to reflect this effect in the Sauter mean diameter correlation [32], and the concept of impeller swept volume (the volume of the cylinder with the same diameter and height as the impeller) was introduced for the correlation [35].

If the volume of the impeller zone was the same as the aforementioned impeller swept volume, there should have been no significant change in the Sauter mean diameter since the sum of the swept volumes of the two impellers remained unchanged when the liquid phase volume was reduced at the fixed top clearance. However, the Sauter mean diameter increased as the whole liquid phase volume decreased. Thus, the change of the droplet size may have been due to a change in the flow pattern, since the flow pattern inside the liquid mixture changed when the impeller spacing varied (impeller spacing decreased as the liquid phase volume decreased with the liquid top clearance fixed) [13,36,37]. According

to the previous studies, the flow pattern produced by each impeller did not overlap and acted independently when the impeller spacing (S) was larger than $2D_I$ [38,39]. When the liquid phase volume was 80 L, the flow patterns did not overlap since S/D_I was 2.42 (Table 2). However, if the liquid phase volume decreased to 69 L, the S/D_I significantly decreased to 1.70, causing the flow pattern produced from the impellers to overlap. In this condition, the flow pattern of one impeller may affect the other. When the liquid phase volume further decreased to 64 L, the S/D_I reached 1.26, resulting in much more overlap between the two flow patterns. This forces the droplets to approach the vicinity of the impeller [40]; but, on the other hand, enhanced internal flow can interfere with the droplet breakup by reducing the residence time of the droplets in the vicinity of impeller. If the latter occurs predominantly, the Sauter mean diameter will increase.

In addition, the flow pattern may be related to the size of the impeller zone. Since significant energy dissipation takes place in the impeller zone [41-43], the volume of the impeller zone should be considered to be more important than the entire liquid phase volume. However, it is unrealistic that the impeller affects the impeller swept volume only. Thus, if the area of the impeller flow pattern (which is much bigger than the impeller swept volume) is assumed to be the impeller zone, an area where the two impeller zones overlap can be created as the impeller spacing decreases. Then, the sum of the two impeller zone volumes becomes smaller than that when each impeller zone is present independently. The overall droplet size is likely to increase as the liquid phase volume decreases, since the decrease in the impeller zone volume means that the region affected by the impeller decreases.

2. Sauter Mean Diameter Measurement at Different Impeller Spacings

Fig. 5 presents the results of the Sauter mean diameter measurement when the impeller spacing changes with the liquid phase volume fixed at 80 L. Regardless of the sampling location and the impeller speed, the Sauter mean diameter was generally the smallest when the impeller spacing was 27.0 cm. When the gap between the two impellers was less than or greater than this, the Sauter mean diameter increased. These results confirmed that the droplet size can vary greatly depending on the relative position or the spacing
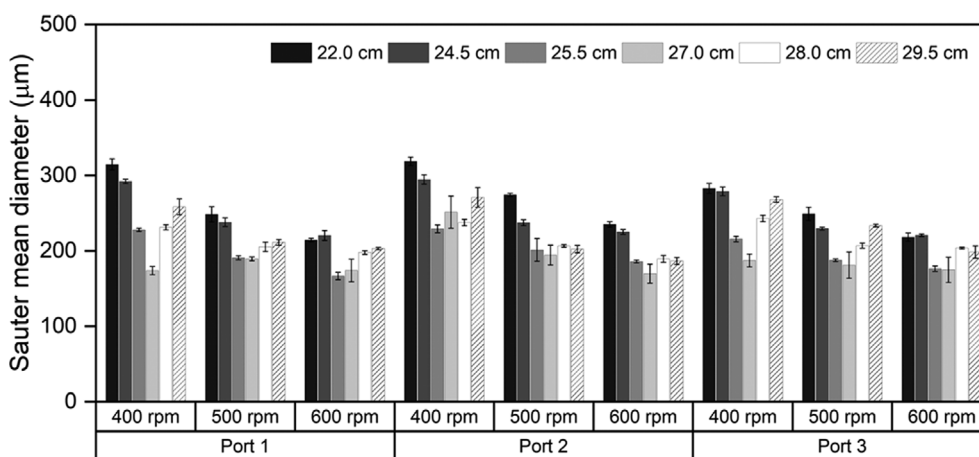

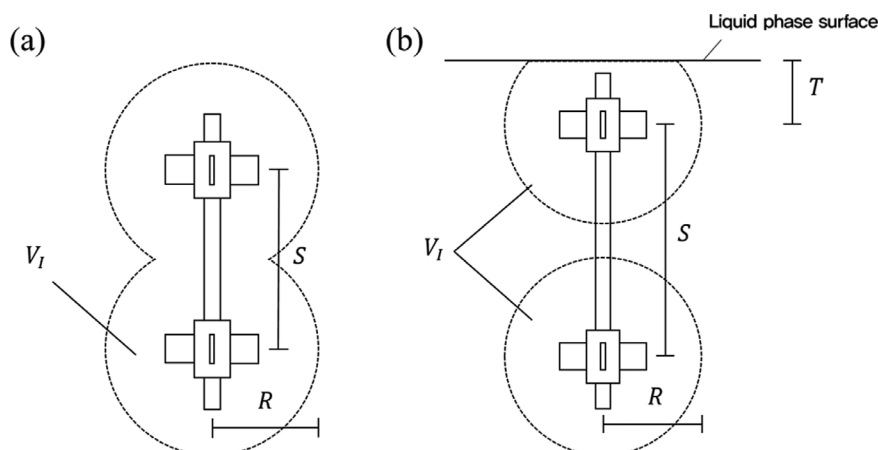Fig. 5. Measured Sauter mean diameters with different impeller spacings.

Fig. 6. Schematic diagram of the impeller zone with varying impeller spacing: (a) for S<27.0 cm; (b) for S>27.0 cm.

of the two impellers, even if the impeller geometry does not change under the fixed liquid phase volume.

The reason why the Sauter mean diameter increases when the impeller spacing is smaller than 27.0 cm seems to be due to the two overlapped impeller zones, as presented in Fig. 6(a). In this case, the total impeller zone volume decreased, and this gives a rough estimate of the size of the impeller zone. Assuming that the smaller impeller zone volume results in a larger droplet size by diminishing the area where the droplet breakup occurs, the radius of each impeller zone could be between 12.75 and 13.50 cm. Thus, if the impeller zone radius is within that range, the two impeller zones begin to overlap when the impeller spacing is decreased from 27.0 cm. Thus, if the impeller zone radius (R) is 12.75 cm, the Sauter mean diameter increases when S<2R (i.e., S<2.28D_I). This does not deviate much from the results of a previous study that the impeller flow patterns of the dual impeller overlaps when S<2D_I [38,39]. Thus, assuming the area of the impeller flow pattern as the impeller zone, its volume change can be used for the estimation of the Sauter mean diameter.

However, if the impeller zone volume affects the droplet size,

the Sauter mean diameter should also increase when the top clearance of the upper impeller is smaller than the impeller zone radius (T<R). In this case, the part of the impeller zone of the upper impeller is cut off by the liquid phase top surface, so the total impeller zone volume decreases as illustrated in Fig. 6(b). Since the top clearance of the upper impeller was 12.7 cm when the impeller spacing was 27.0 cm (Table 2), the total volume of the impeller zone would decrease immediately if the upper impeller moved upward in these conditions (under the assumption that the R ranges from 12.75 to 13.50 cm, it satisfies T<R). Therefore, the Sauter mean diameter should increase if the sum of the impeller zone volume affected the droplet size, and it actually increased when the impeller spacing was greater than 27.0 cm (i.e., T<12.7 cm, which is the same as T<1.14D_I). Thus, if the area of the flow pattern produced by an impeller is assumed to be an impeller zone, it is confirmed that the impeller zone volume is inversely proportional to the measured Sauter mean diameter.

3. Sauter Mean Diameter Measurement at Different Dual Impeller Designs

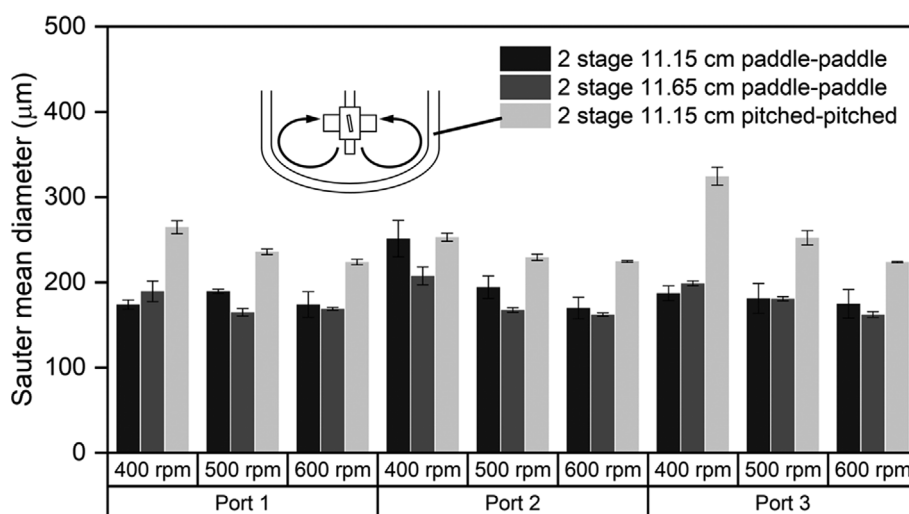Under a fixed liquid phase volume, the diameter and the blade

Fig. 7. Measured Sauter mean diameters with different dual impeller designs.

angle of the two-stage impellers (dual impeller system) were changed, and the resulting Sauter mean diameters are shown in Fig. 7. When the impeller diameter was 11.15 cm, the droplet size did not decrease significantly even if the impeller speed increased. Therefore, by increasing the impeller diameter, it was confirmed whether the Sauter mean diameter in these conditions reached its minimum. As the diameter of the paddle-paddle impeller increased from 11.15 to 11.65 cm, the Sauter mean diameter generally decreased. Thus, the droplet size could be further reduced by increasing the impeller diameter, and even a slight increase in the impeller diameter can have a significant effect on the droplet size. It was also confirmed that the increase in impeller diameter affected not only the droplets located near ports 1 or 3 (vicinity of the impeller), but also the droplets near port 2.

With regard to the effect of the impeller blade angle, the Sauter mean diameter increased when both the paddle impellers were replaced with the 10° pitched paddle impellers. As the impeller speed increased, the deviation of the Sauter mean diameter by the sampling location was greatly reduced, and the droplet size uniformity was enhanced. According to the previous study, using the axial flow impeller at the top and the radial flow impeller at the bottom showed the highest performance of the droplet size uniformity in the dual impeller system [20]. Therefore, the mixing performance may not increase so much if two pitched paddle impellers (i.e., two axial flow impellers) are used. However, since the reactor bottom used in this study was a dished form, the secondary flow might have spread upward through the reactor bottom wall (Fig. 7), which could help the droplet size to be homogenized. In fact, in the stirred tank for a solid suspension, the axial flow impeller located near the reactor bottom is known to have the effect of moving the solid at the bottom upwards [44]. Thus, this effect can also be expected in the case of droplets. After replacing the lower paddle impeller with the pitched paddle, the axial flow became much stronger, and it can create an intensified secondary flow. This may result in the enhanced droplet size uniformity due to the intensified mixing performance.

For the case where one more paddle impeller was added to port 2, the Sauter mean diameter at each sampling location and impeller speed is shown in Fig. 8. Even when the impeller power consumption increased largely due to the addition of the impeller, the Sauter mean diameter slightly increased. Especially for port 2, the Sauter mean diameter increased, even though it was the region most affected by the newly added impeller.

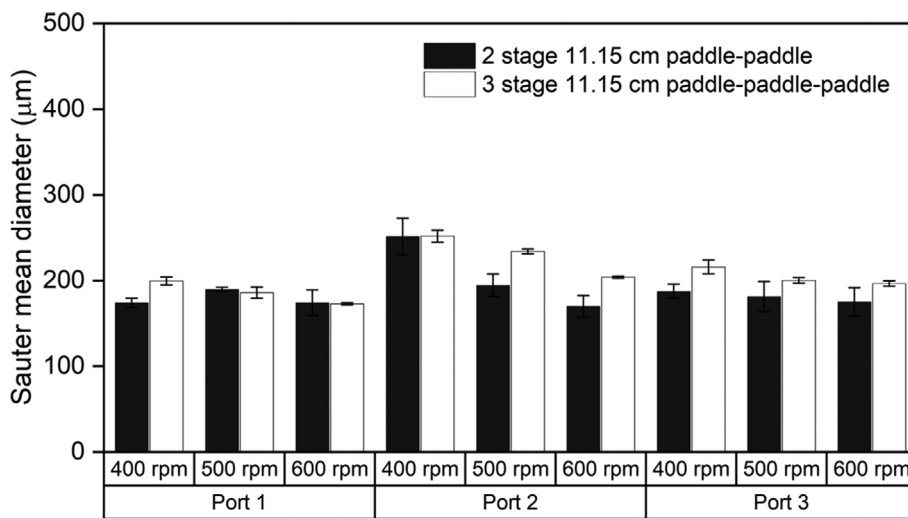This can be explained by the relation between the droplet size

Fig. 8. Measured Sauter mean diameters with different impeller stage numbers.
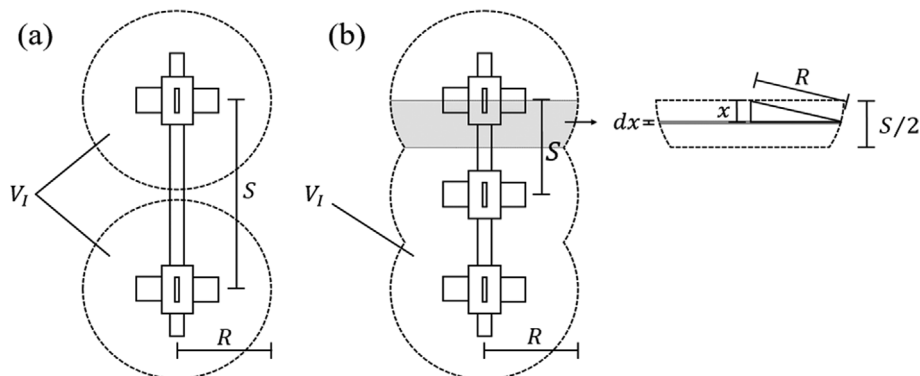

Fig. 9. Schematic diagram of the impeller zone: (a) for 2 stage paddle impellers; (b) for 3 stage paddle impellers.

and the area of the flow pattern produced by the impeller, as seen in Section 3.2. Fig. 9 provides a schematic diagram of the impellers and impeller zones for both the impellers. The addition of the new impeller to port 2 greatly reduced the impeller spacing to 13.5 cm. In Section 3.2, the impeller zone radius (R) of the paddle impeller with a 11.15 cm diameter was 12.75-13.50 cm. Thus, the impeller zone volume (V_I) for each impeller can be calculated as presented in Eq. (3).

$$\text{2 stage paddle impellers: } V_I = 2 \times \frac{4}{3}\pi R^3$$
$$\text{3 stage paddle impellers: } V_I = \frac{4}{3}\pi R^3 + 4 \times \int_0^{S/2} \pi(R^2 - x^2)dx \qquad (3)$$

When R=12.75 cm, the total impeller zone volume increased from 17.36 to 21.18 L (22.00% increase) when the number of impellers increased to three. When R=13.50 cm, the increase in the impeller zone volume with the three impellers was 18.75% (20.61 to 24.48 L). Thus, the increase in the total impeller zone volume was small, considering that the addition of the new impeller significantly increased the total impeller power consumption. However, when the distance between the impellers was too small, the residence time of the droplets at the one impeller zone decreased due to the intensified flow produced by the other adjacent impeller. Thus, the droplet breakup effect did not increase much since the droplet residence time in the vicinity of the impeller largely decreased, resulting in a large droplet size.

Then the question arises as to whether the droplet size will always increase even when the number of impellers continuously increases. If the number of impellers increases significantly and the impeller spacings are reduced to an extreme level, the flow patterns produced by each impeller will go beyond the level of overlap and become indistinguishable. According to Hudcova et al. [38], when the two impeller blades are completely adjacent, the flow pattern is the same as with a single impeller with a doubled blade width. In addition, the power consumption increased only by 30% over the single one. Therefore, if the number of impellers increases enough, it will be difficult to reduce the residence time of the droplets at the impeller zone, because the flow patterns of the impellers no longer affect each other since the impellers are indistinguishable. In this case, however, the total power consumption will somehow increase as the number of impellers increases, so the Sauter mean diameter is expected to decrease eventually.

4. Effect of Various Multi-stage Impeller Designs on the Droplet Size Uniformity

The Sauter mean diameter is a very useful parameter to evaluate the productivity of the stirred tank, but it only shows the fragmentary effect of the droplet breakup and does not show the droplet size distributions under certain conditions [13]. Thus, for the impeller designs covered in Sections 3.2 and 3.3, the actual droplet sizes obtained through the measurements were shown using a box plot, and the results are presented in Fig. 10.

In Fig. 10(a), when the dual paddle impeller was used and the impeller diameter increased from 11.15 to 11.65 cm, the deviation between the droplet sizes in the central 50% area of the total droplet size decreased significantly (2S-11.65-PAD), since the height of the box decreased. This shows that the increase in the impeller
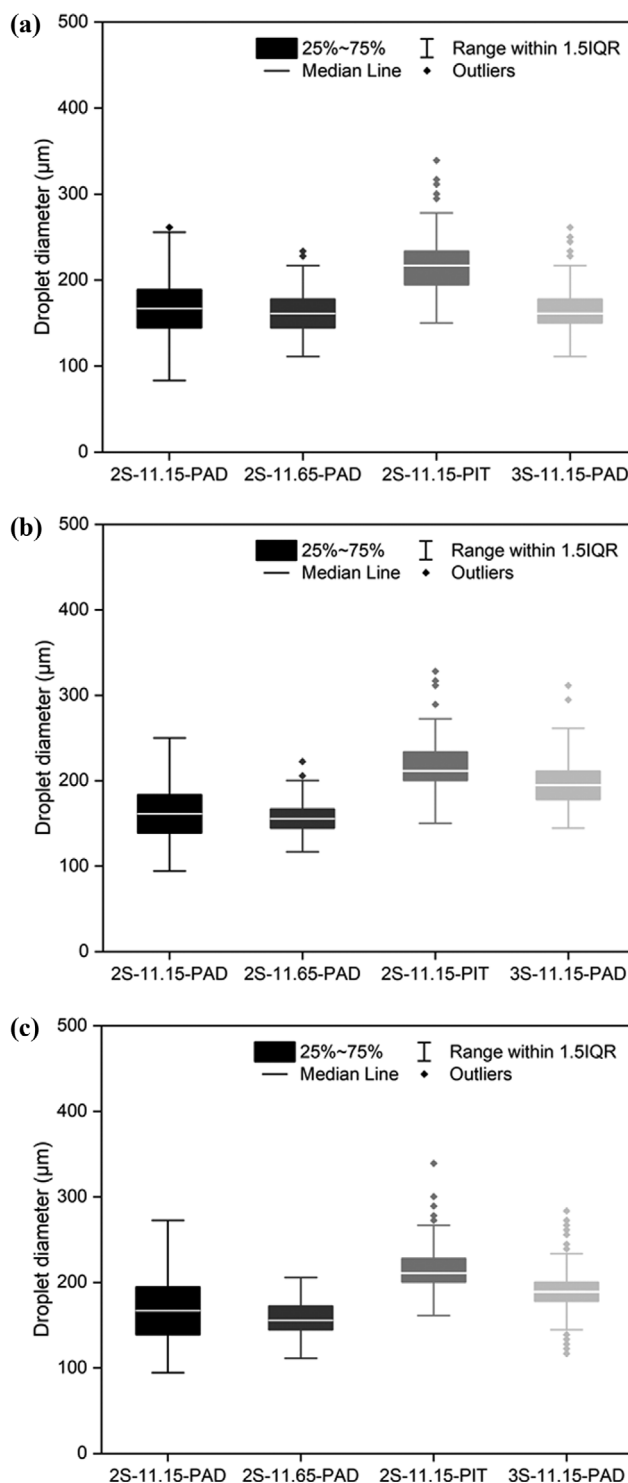

Fig. 10. Box plot diagram of the droplet size distributions for the different multiple impeller designs: (a) at port 1; (b) at port 2; (c) at port 3.

diameter not only decreased the Sauter mean diameter, but also increased the droplet size uniformity. The range of the central 50% area slightly decreased when both paddle impellers were replaced by 10° pitched paddles, confirming that the droplet size uniformity was enhanced despite the increase in the Sauter mean diame-

ter (2S-11.15-PIT). Finally, when the three-stage paddle impeller was used (3S-11.15-PAD), the deviation between the droplet sizes was the lowest. This appears to have been due to the flow caused by the addition of the impeller, which seemed to have greatly increased the mixing efficiency. Thus, the droplet size uniformity increased when the diameter, blade angle, and number of impellers increased, but that did not always indicate the Sauter mean diameter decrease.

For port 2, as shown in Fig. 10(b), the deviation of the droplet sizes was greatly reduced as the diameter of the dual paddle impeller increased (2S-11.65-PAD). Despite the absence of an impeller nearby, it could be confirmed that increasing the diameter of the upper and lower impellers would be of great help in enhancing droplet size uniformity. Similarly, the deviation between the droplet sizes was reduced when the two paddle impellers were replaced by two 10° pitched paddle impellers (2S-11.15-PIT). This seemed to occur because the droplets located in port 2 were more affected by the downward flow than the droplets in port 1. The increase in the number of paddle impellers to three also increased the degree of the droplet size uniformity (3S-11.15-PAD), when compared with the dual impeller case.

As shown in Fig. 10(c), a similar pattern appeared at port 3. Note that the deviation between the droplet sizes at port 3 was smaller than that of port 2 when two 10° pitched paddle impellers were used (2S-11.15-PIT), which were affected by both the downward flow of the upper pitched paddle and the secondary flow produced by the lower pitched paddle. In addition, it was also confirmed that the use of three paddle impellers produced the most enhanced uniformity of droplet size.

Thus, the deviation between the droplet sizes could be reduced by increasing the diameter and the number of impellers, or intensifying the axial flow by increasing the impeller blade angle. However, increasing the number of impellers did not always show the best degree of droplet size uniformity, even though it had the highest power consumption among the impeller systems used in this study. Therefore, to reduce the deviation between the droplet sizes, increasing the impeller diameter or the blade angle is helpful, but the increase or decrease effect of the Sauter mean diameter under such conditions should be considered together to select the proper impeller designs.

CONCLUSIONS

This study measured the Sauter mean diameter and the droplet size distribution in a stirred tank by changing the liquid phase volume, impeller spacing, dual impeller design, and the number of impellers. By using a borescope method, droplet images were successfully obtained and the effect of multiple impeller designs and configurations was investigated. When the liquid phase volume decreased, the Sauter mean diameter increased even though the power per volume remained constant. Assuming the area of the flow pattern produced by the impeller as an impeller zone, its volume was inversely proportional to the Sauter mean diameter. Thus, as the liquid phase volume decreased, the Sauter mean diameter increased due to the overlap of the flow pattern. When the liquid phase volume was fixed and the impeller spacing was varied, the

Sauter mean diameter increased as the impeller zone overlapped ($S<2.28D_I$) or the upper impeller moved too upward ($T<1.14D_I$). Finally, the change of the Sauter mean diameter and the droplet size uniformity was studied when the impeller diameter, blade angle, and the number of impellers were varied. In all three cases, the droplet size uniformity increased, but that did not always mean a decreased Sauter mean diameter. When the impeller blade angle increased, the Sauter mean diameter increased significantly, while it decreased when the impeller diameter increased.

NOMENCLATURE

Symbols Used

B   : bottom clearance of the lower impeller [cm]
D   : reactor diameter [cm]
D_I : impeller diameter [cm]
d_i : droplet diameter [cm]
d_{32} : Sauter mean diameter [cm]
H   : liquid phase height [cm]
M   : torque of the impeller [N m]
N   : impeller speed [s^{-1}]
N_I : number of impellers [-]
n_i : number of droplets
P   : power consumption [W]
R   : impeller zone radius [cm]
S   : impeller spacing [cm]
T   : top clearance of the upper impeller [cm]
V   : liquid phase volume [L]
V_I : impeller zone volume [L]
W   : impeller blade width [cm]

Greek Symbols

$\bar{\varepsilon}$: mean energy dissipation rate [W kg^{-1}]
θ : impeller blade angle of the upper impeller [°]
ϕ : organic phase holdup [-]

SUPPORTING INFORMATION

Additional information as noted in the text. This information is available via the Internet at http://www.springer.com/chemistry/journal/11814.

REFERENCES

1. C. Joshi and R. S. Singhal, *Korean J. Chem. Eng.*, **35**, 195 (2018).
2. H. Im, J. Park and J. W. Lee, *Korean J. Chem. Eng.*, **36**, 1680 (2019).
3. J. W. Lee, Y. C. Ko, Y. K. Jung, K. S. Lee and E. S. Yoon, *Comput. Chem. Eng.*, **21**, S1105 (1997).
4. J.-R. Lee, N. Hasolli, K.-S. Lee, K.-Y. Lee and Y.-O. Park, *Korean J. Chem. Eng.*, **36**, 1548 (2019).
5. A. Wongkia, K. Suriye, A. Nonkhamwong, P. Praserthdam and S. Assabumrungrat, *Korean J. Chem. Eng.*, **30**, 593 (2013).
6. J. A. Rocha-Valadez, M., Hassan, G. Corkidi, C. Flores, E. Galindo and L. Serrano-Carreón, *Biotechnol. Bioeng.*, **91**, 54 (2005).
7. D. E. Bergbreiter and S. D. Sung, *Adv. Synth. Catal.*, **348**, 1352 (2006).

8. J. Park, S. Lee and J. W. Lee, *Ind. Eng. Chem. Res.*, **57**, 2310 (2018).

9. J. H. Lee, H. U. Lee, J. H. Lee, S. K. Lee, H. Y. Yoo, C. Park and S. W. Kim, *Korean J. Chem. Eng.*, **36**, 71 (2019).

10. C. Desnoyer, O. Masbernat and C. Gourdon, *Chem. Eng. Sci.*, **58**, 1353 (2003).

11. M. Kraume, A. Gäbler and K. Schulze, *Chem. Eng. Technol.*, **27**, 330 (2004).

12. S. Lee and A. Varma, *AIChE J.*, **61**, 2228 (2015).

13. L. Böhm, L. Hohl, C. Bliatsiou and M. Kraume, *Chem. Ing. Tech.*, **91**, 1724 (2019).

14. A. Gäbler, M. Wegener, A. Paschedag and M. Kraume, *Chem. Eng. Sci.*, **61**, 3018 (2006).

15. D. Pinelli, A. Bakker, K. Myers, M. Reeder, J. Fasano and F. Magelli, *Chem. Eng. Res. Des.*, **81**, 448 (2003).

16. S. Maaß, T. Rehm and M. Kraume, *Chem. Eng. J.*, **168**, 827 (2011).

17. N. Hardy, F. Augier, A. W. Nienow, C. Béal and F. B. Chaabane, *Chem. Eng. Sci.*, **172**, 158 (2017).

18. D. Gu, Z. Liu, C. Xu, J. Li, C. Tao and Y. Wang, *Chem. Eng. Process.*, **118**, 37 (2017).

19. V. Mishra and J. Joshi, *Chem. Eng. Res. Des.*, **72**, 657 (1994).

20. M. Cai, X. Zhou, J. Lu, W. Fan, C. Niu, J. Zhou, X. Sun, L. Kang and Y. Zhang, *Bioresour. Technol.*, **102**, 3584 (2011).

21. F. Magelli, G. Montante, D. Pinelli and A. Paglianti, *Chem. Eng. Sci.*, **101**, 712 (2013).

22. R. Darvishi, M. N. Esfahany and R. Bagheri, *Ind. Eng. Chem. Res.*, **54**, 10953 (2015).

23. M. Ruiz, P. Lermanda and R. Padilla, *Hydrometallurgy*, **63**, 65 (2002).

24. J. Ritter and M. Kraume, *Chem. Eng. Technol.*, **23**, 579 (2000).

25. W. M. Haynes, D. R. Lide and T. J. Bruno, *CRC handbook of chemistry and physics*, CRC Press, Boca Raton, Florida (2017).

26. M. Laliberté, *J. Chem. Eng. Data*, **52**, 321 (2007).

27. N. Vargaftik, B. Volkov and L. Voljak, *J. Phys. Chem. Ref. Data*, **12**, 817 (1983).

28. H. Girault, D. Schiffrin and B. Smith, *J. Colloid Interface Sci.*, **101**, 257 (1984).

29. J. Lovick, A. Mouza, S. Paras, G. Lye and P. Angeli, *J. Chem. Technol. Biotechnol.*, **80**, 545 (2005).

30. B. Letellier, C. Xuereb, P. Swaels, P. Hobbes and J. Bertrand, *Chem. Eng. Sci.*, **57**, 4617 (2002).

31. S. Okufi, E. P. De Ortiz and H. Sawistowski, *Can. J. Chem. Eng.*, **68**, 400 (1990).

32. P. Jüsten, G. Paul, A. Nienow and C. Thomas, *Biotechnol. Bioeng.*, **52**, 672 (1996).

33. G. Zhou and S. M. Kresta, *Chem. Eng. Sci.*, **53**, 2063 (1998).

34. A. Amanullah, B. C. Buckland and A. W. Nienow, *Handbook of industrial mixing: Science and practice*, John Wiley & Sons Inc., Hoboken, New Jersey, 1071 (2004).

35. W. McManamey, *Chem. Eng. Sci.*, **34**, 432 (1979).

36. K. Rutherford, K. Lee, S. Mahmoudi and M. Yianneskis, *AIChE J.*, **42**, 332 (1996).

37. P. R. Gogate, A. A. Beenackers and A. B. Pandit, *Biochem. Eng. J.*, **6**, 109 (2000).

38. V. Hudcova, V. Machon and A. Nienow, *Biotechnol. Bioeng.*, **34**, 617 (1989).

39. C. Baudou, C. Xuereb and J. Bertrand, *Can. J. Chem. Eng.*, **75**, 653 (1997).

40. A. Pacek, S. Chamsart, A. Nienow and A. Bakker, *Chem. Eng. Sci.*, **54**, 4211 (1999).

41. L. A. Cutter, *AIChE J.*, **12**, 35 (1966).

42. H. Wu and G. Patterson, *Chem. Eng. Sci.*, **44**, 2207 (1989).

43. J. Sheng, H. Meng and R. Fox, *Chem. Eng. Sci.*, **55**, 4423 (2000).

44. E. L. Paul, V. A. Atiemo-Obeng and S. M. Kresta, *Handbook of industrial mixing: Science and practice*, John Wiley & Sons Inc., Hoboken (2004).